RSC Advances

PAPER

View Article Online
View Journal | View Issue

Cite this: *RSC Adv.*, 2017, **7**, 45495

Heteropolytungstostannate as a homo- and heterogeneous catalyst for Knoevenagel condensations, selective oxidation of sulfides and oxidative amination of aldehydes

Roushan Khoshnavazi,* Leila Bahrami and Manuchehr Rezaei

Received 1st June 2017
Accepted 9th September 2017

DOI: 10.1039/c7ra06112a

rsc.li/rsc-advances

Heteropolytungstostannate $K_{11}H[P_2W_{18}O_{68}(HOSn^{IV}OH)_3]\cdot 20H_2O$ (**1**) is used as a homo- and heterogeneous catalyst for Knoevenagel condensations. New $Fe_3O_4@SiO_2@CH_2(CH_2)_2NH_3^+$-$[P_2W_{18}O_{68}(HOSn^{IV}OH)_3]^{11-}$ nanocatalyst was fabricated through electrostatic grafting of (**1**) on amine-modified silica-coated magnetic nanoparticles. The new magnetically recoverable nanocatalyst was characterized using infrared spectroscopy (IR), scanning electron microscopy (SEM), transmission electron microscopy (TEM), X-ray powder diffractometry (XRD), energy-dispersive X-ray analysis (EDX) and alternating gradient force magnetometry (AGFM). The results indicate that the particles are mostly spherical in shape and have an average size of approximately <30 nm. The catalytic activity of the catalyst was investigated in the selective oxidation of sulfides to sulfoxides and oxidative amination of aldehydes in an aqueous medium. The catalyst was reused at least five times without significant decrease in catalytic activities, and the structure of the catalyst remained unchanged after recycling.

Introduction

Polyoxometalates (POMs) are a large class of molecular metal-oxide clusters with unmatched structural variety and versatility properties. POMs due to diversity in structure and composition have been used in many fields, including catalysis, medicine and material science.[1–4] Owing to their redox and acidic properties, POMs exhibit catalytic activity in both homogeneous and heterogeneous catalysis.[5,6] The application of POMs as catalysts is limited because they are solids with a low surface area (less than 10 $m^2\ g^{-1}$) and also have high solubility in polar solvents. To overcome the limitations, POMs have been supported on inert and high-surface-area materials. Self-assembly techniques are being developed for designing catalysts based on polyoxometalates such as self-assembly of polyoxometalate with cations and positively charged nanoparticles that could facilitate catalyst recycling *via* filtration or centrifugation.[7–11] Recently, magnetic nanoparticles (MNPs) have become promising candidates as high-surface-area materials for immobilization of homogeneous catalysts.[12,13] Owing to their exceptionally high surface areas, MNPs exhibit high activity under mild conditions. Most examples of immobilization of POMs on surfaces have been limited to non-covalent interactions between Keggin heteropolyacids through electrostatic interaction of external oxygen atoms of the POMs with protonated hydroxyl groups of the surface.

In comparison with the Keggin and Dawson-type POMs, the catalytic properties of sandwich-type POMs as heterogeneous catalysts have not been extensively studied.[14–17] In this research, we investigate the catalytic properties of tin-containing sandwich-type polyoxometalates $[P_2W_{18}O_{68}(HOSn^{IV}OH)_3]^{12-}$. The structure of $[P_2W_{18}O_{68}(HOSn^{IV}OH)_3]^{12-}$ (**1**) consists of two A-type α-PW_9O_{34} anions linked by three tin(IV) cations leading to A-type sandwich POM[18] (Fig. 1). Tin-containing sandwich-type polyoxometalates are more hydrolytically stable than transition-metal-substituted sandwich-type polyoxometalates in aqueous solution[18–20] and thus are more suitable for oxidation reactions. Encouraged by these results, we evaluated the interaction of **1** with already prepared amine-modified silica-coated magnetite nanoparticles. The catalytic activity of the tin-containing sandwich-type polyoxometalate and the prepared nanocomposite was examined in reactions such as Knoevenagel condensations, oxidation of sulfides with H_2O_2 and oxidative amination of aldehydes in a green medium.

Experimental section

Materials

All reagents were commercially obtained from Merck chemical company, Acrōs Organics and Sigma-Aldrich and used without further purification. Heteropolytungstostannate $K_{11}H[P_2W_{18}O_{68}(HOSn^{IV}OH)_3]\cdot 20H_2O$ was prepared according to the

Department of Chemistry, University of Kurdistan, P.O. Box 66135-416, Sanandaj, Iran. E-mail: r.khoshnavazi@uok.ac.ir; khoshnavazi@yahoo.com; Fax: +98 8733 624 133; Tel: +98 8733 624 133

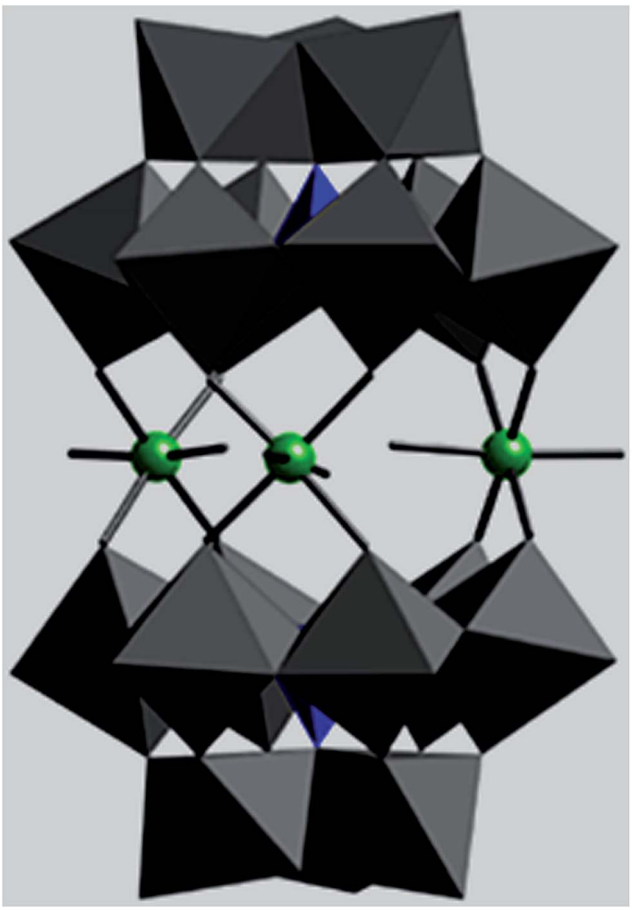

Fig. 1 Polyhedral representation of $[P_2W_{18}O_{68}(HOSn^{IV}OH)_3]^{12-}$.

literature.[18] The Fe_3O_4 nanoparticles, silica-coated magnetite nanoparticles (Fe_3O_4@SiO_2) and Fe_3O_4@$SiO_2CH_2(CH_2)_2NH_2$ were prepared according to the literature.[21–23]

Characterization

The crystal structure of the synthesized nanocomposite was characterized by a Philips (X'Pert MPD) diffractometer in 40 kV and 30 mA with a CuKα radiation (λ = 1.5418 Å). Infrared spectra were recorded on a Bruker Vector 22 FT-IR using KBr pellet. The morphology of nanocomposite was revealed using a scanning electron microscope (FESEM-TESCAN MIRA3 from Czech Republic) and a transmission electron microscope (TEM, Zeiss-EM10C 80 KV).

The elements in the nanocomposite sample were probed using energy-dispersive X-ray (EDX) spectroscopy accessory to the FESEM-TESCAN MIRA3 scanning electron microscopy. The magnetic properties were investigated using a home-made alternative gradient force magnetometer (AGFM) in the magnetic field range of −5000 to 5000 Oe at room temperature. Textural characteristics of the outgassed samples were obtained from nitrogen physisorption at 77 K using a Brunauer, Emmett and Teller surface area and porosity analyzer instrument.

Synthesis

Magnetic nanoparticle-supported polyoxometalate

*Fe_3O_4@SiO_2@$CH_2(CH_2)_2NH_3^+[P_2W_{18}O_{68}(HOSn^{IV}OH)_3]^{11-}$ (**1a**).* Fe_3O_4@$SiO_2CH_2(CH_2)_2NH_2$ (0.1 g) was dispersed in 20 mL of deionized water and ultrasonicated for 30 min. Then, a solution of **1** (0.1 g in 5 mL deionized water) was added dropwise into the solution, ultrasonicated for 30 min and the mixture was stirred under reflux condition for 24 h. The obtained solid was then magnetically collected from the solution and washed abundantly with water/ethanol and dried at 60 °C.

Typical procedures for catalytic experiments

The Knoevenagel condensations. In a typical experiment, aldehyde (1 mmol) and malononitrile (1.2 mmol), 0.010 g of **1** as catalyst and water or ethanol (1 mL) were placed in a 20 mL glass bottle at 25 °C. The reaction mixture was constantly stirred vigorously. The progress was monitored through TLC (eluent: *n*-hexane/EtOAc, 2 : 1). After completion of the reaction, the reaction mixture was transferred to a separating funnel and EtOAc (3 × 5 mL) was added and then the products were separated. After evaporation of EtOAc, the obtained products were recrystallized from EtOH and pure products were obtained in 85–95% yield.

The oxidation of sulfides to sulfoxides. The catalytic activity of the catalyst was investigated in the selective oxidation of sulfides to sulfoxides using 30% H_2O_2 as a green oxidant. A mixture containing a sulfide (1 mmol), H_2O (1.25 mL), 30% H_2O_2 (6 mmol) and catalyst **1a** (0.030 g) was stirred at room temperature for the time specified. The progress of the reaction was monitored through TLC (eluent: *n*-hexane/EtOAc, 2 : 1). After completion of the reaction, the catalyst was separated from the product using an external magnet. The product was extracted with CH_2Cl_2 (3 × 5 mL) and the combined organics were washed with brine (10 mL) and dried over anhydrous Na_2SO_4. The solvent was removed under reduced pressure to afford the corresponding pure sulfoxide in most cases.

The oxidative amination of aldehydes. While stirring aldehyde (1 mmol), hydroxylamine hydrochloride (1.2 mmol) and $NaHCO_3$ (1.2 mmol) in water (1 mL), **1a** nanocatalyst (0.020 g) was added to the mixture at a temperature of 90 °C. After completion of the reaction and separation of the magnetic nanocatalyst using an external magnet, the reaction mixture was extracted with ethyl acetate and washed with brine and then dried with Na_2SO_4. For further purification, the products were recrystallized from hexane and dichloromethane mixture to afford the desired products. The obtained products were identified on comparison of the physical properties and spectral data with pure samples and those reported in the literature.

Results and discussion

Synthesis and characterization

Magnetic Fe_3O_4 nanoparticles were prepared by chemical co-precipitation of Fe^{2+} and Fe^{3+} ions in the basic solution and silica-coated magnetite nanoparticles were prepared by the Stöber method.[21] The Fe_3O_4@$SiO_2CH_2(CH_2)_2NH_2$ nanoparticle was prepared by covalent grafting of silanol groups of Fe_3O_4@SiO_2 surface and 3-aminopropyltriethoxysilane (APTS).

Magnetic nanoparticles of **1a** was prepared by simple direct addition of heteropolytungstostannate of $[P_2W_{18}O_{68}(HOSn^{IV}OH)_3]^{12-}$ aqueous solution to $Fe_3O_4@SiO_2CH_2(CH_2)_2NH_2$ nanoparticle. The magnetic nanoparticle of $Fe_3O_4@SiO_2@CH_2(CH_2)_2NH_2$ was protonated by the acidic hydrogen and the hydrogen of hydroxide groups in the structure of $K_{11}H[P_2W_{18}O_{68}(OHSn^{IV}OH)_3]\cdot 20H_2O$. The anionic $[P_2W_{18}O_{68}(OHSn^{IV}OH)_3]^{12-}$ was attached to positively charged magnetic nanoparticles, $Fe_3O_4@SiO_2@CH_2(CH_2)_2NH_3^+$ nanoparticle through electrostatic interactions. The nanocatalyst synthesis pathway is shown in Scheme 1.

FT-IR spectra of **1a**, $Fe_3O_4@SiO_2CH_2(CH_2)_2NH_2$ and **1** are shown in Fig. 2. The peak at 573 cm^{-1} in $Fe_3O_4@SiO_2CH_2(CH_2)_2NH_2$ and **1a** spectra could be attributed to Fe–O stretching vibration.[24] Two bands at 1070 and 800 cm^{-1} are ascribed to the symmetrical and asymmetrical vibrations of the Si–O–Si bonds.[25] The very strong bands appearing in the 700–1090 cm^{-1} in spectrum of **1a** are clearly assigned to W–O–W, W=O and P–O stretching modes of $[P_2W_{18}O_{68}(HOSn^{IV}OH)_3]^{12-}$. The results show that small shifts to the higher wavenumbers were observed compared to 1. The C–H stretching vibration bands of the anchored propyl group appeared at 2925 and 2850 cm^{-1}.[26] These results prove the formation of nanocomposite **1a**.

Fig. 3 shows the XRD results of Fe_3O_4 (a), **1a** (b), and **1** (c). Diffraction peaks with $2\theta = 18.2°$, 30.2°, 35.6°, 43.2°,53.7°, 57.2°, 62.7° and 74.4° are attributed to Fe_3O_4, which indicates a cubic structure of the magnetite.[27] The peaks corresponding to **1** are also observed in **1a**, which is a confirmation of the successful synthesis of nanocomposite. The particle diameters that were calculated from the Scherrer formula are in the range of 18–30 nm.

The EDX spectrum obtained for **1a** (Fig. 4) revealed that Fe, O, Si, C, N, Sn, P and W peaks are associated with $Fe_3O_4@SiO_2@CH_2(CH_2)_2NH_3^+[P_2W_{18}O_{68}(HOSn^{IV}OH)_3]^{11-}$. These results demonstrate that the mentioned polyoxometalate was immobilized onto the surface of the functionalized support.

Magnetic properties of $Fe_3O_4@SiO_2CH_2(CH_2)_2NH_2$ and **1a** nanocomposite were analyzed using an alternating gradient force magnetometer (AGFM) at room temperature (Fig. 5). A decrease in saturation magnetization was observed for **1a**, which could be attributed to the increased mass of $[P_2W_{18}O_{68}(HOSn^{IV}OH)_3]^{12-}$. Even with this reduction in the saturation magnetization, complete magnetic separation of **1a** was achieved in <20 s by placing a magnet near the vessels containing the aqueous dispersion of the nanoparticles. These results indicate the polyoxometalate coating on the magnetic support.

The SEM images show the morphological features of **1a**, which confirm that the nanoparticles were almost spherical (Fig. 6). The nanocomposite shows uniform shape with a mean size less than 30 nm, which is consistent with the XRD results. Magnetic interactions occur between the nanoparticles, which leads to some particle aggregations as shown in the SEM images.

Nitrogen adsorption–desorption isotherms of **1a** nanocomposite show a type IV isotherm with a type H1 hysteresis loop in the high range of relative pressure (Fig. 7A(a)). For the values of high relative pressure, condensation takes place giving a sharp

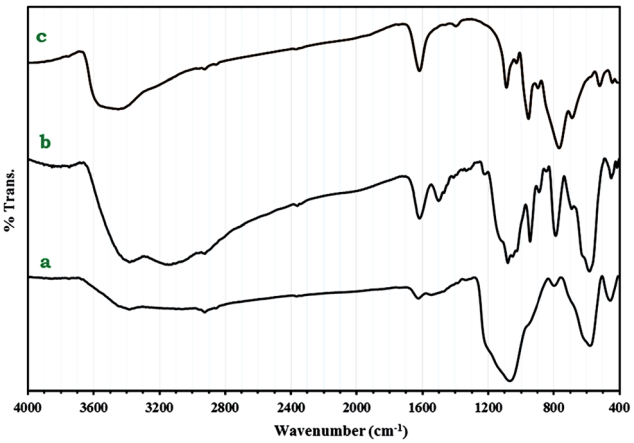

Fig. 2 IR spectra of $Fe_3O_4@SiO_2CH_2(CH_2)_2NH_2$ (a), **1a** nanocomposite (b) and **1** (c).

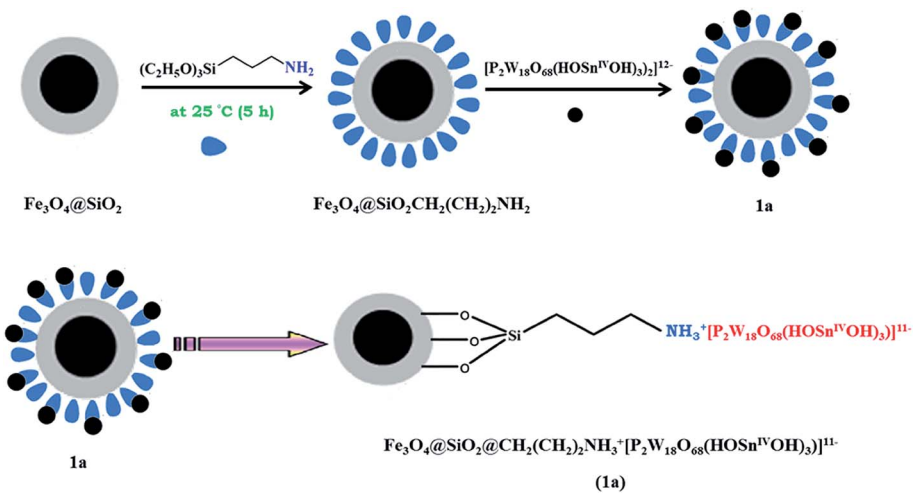

Scheme 1 The synthesis pathway for preparation of **1a** nanocomposite.

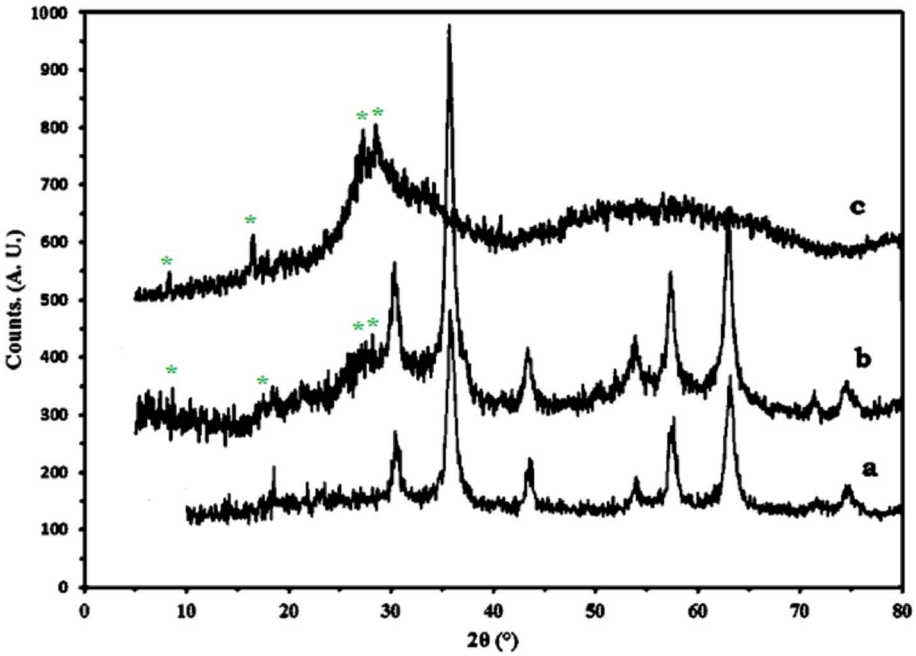

Fig. 3 The XRD diffraction patterns of Fe_3O_4 (a) **1a** nanocomposite (b) and **1** (c).

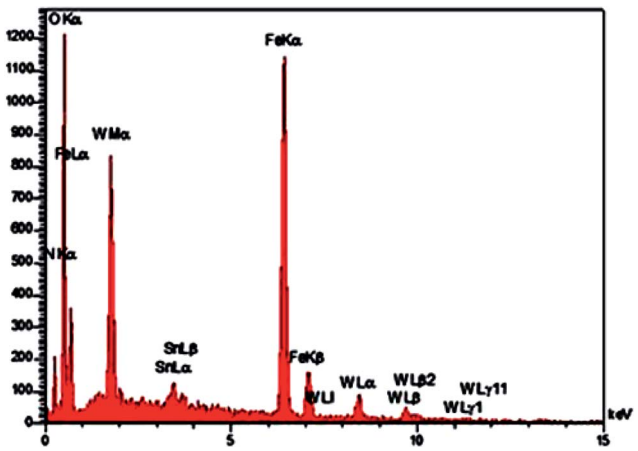

Fig. 4 EDX analysis of **1a** nanocomposite.

adsorption volume increase, which confirms a mesoporous character for **1a** (specific BET surface area, 56.99 $m^2\ g^{-1}$).

The pore size distributions were calculated using the Barret–Joyner–Halenda (BJH) method applied to the adsorption branches of the isotherms. Fig. 7B(a) shows the pore size distribution for **1a** nanocomposite. As shown in the figure a hierarchical set of pores centered near 50 Å and 80 Å (the average pore diameter 96.99 Å) could be observed in the nanocomposite. As expected, the surface area of the crystallite $K_{11}H[P_2W_{18}O_{68}(HOSn^{IV}OH)_3]\cdot 20H_2O$ (**1**) is very small (BJH adsorption cumulative surface area of pores, 5.318 $m^2\ g^{-1}$). The BET analysis illustrates that surface area of **1** markedly increased by immobilization on silica-coated magnetite nanoparticles of Fe_3O_4@$SiO_2CH_2(CH_2)_2NH_2$. The nitrogen adsorption–desorption isotherms and the pore size distribution of the bulk $K_{11}H[P_2W_{18}O_{68}(HOSn^{IV}OH)_3]\cdot 20H_2O$ (**1**) are shown in Fig. 7A(b) and B(b), respectively.

The catalytic applications

The catalytic applications of (1) in the Knoevenagel condensation. First, in this study, the catalytic activity of tin(IV)-containing POM of **1** was examined in Knoevenagel condensations. We found that **1** catalyzes Knoevenagel condensation as a heterogeneous and homogeneous catalyst under mild conditions. The Knoevenagel reaction is one of the most important reactions to form C–C bonds for preparing key derivatives in

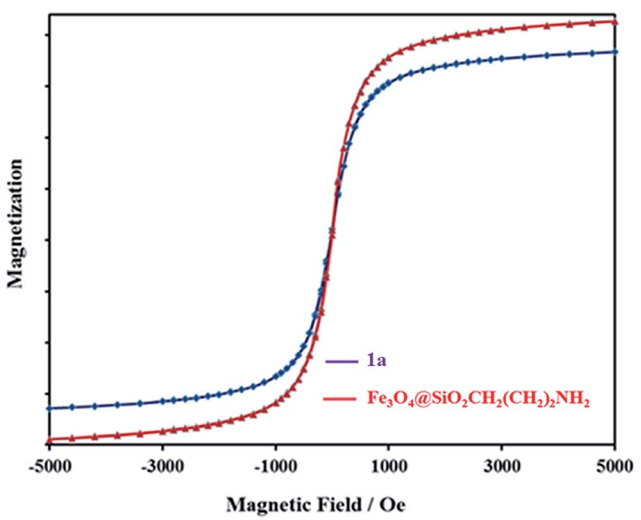

Fig. 5 Alternating gradient force magnetometer (AGFM) of Fe_3O_4@-$SiO_2CH_2(CH_2)_2NH_2$ and **1a** nanocomposite at room temperature.

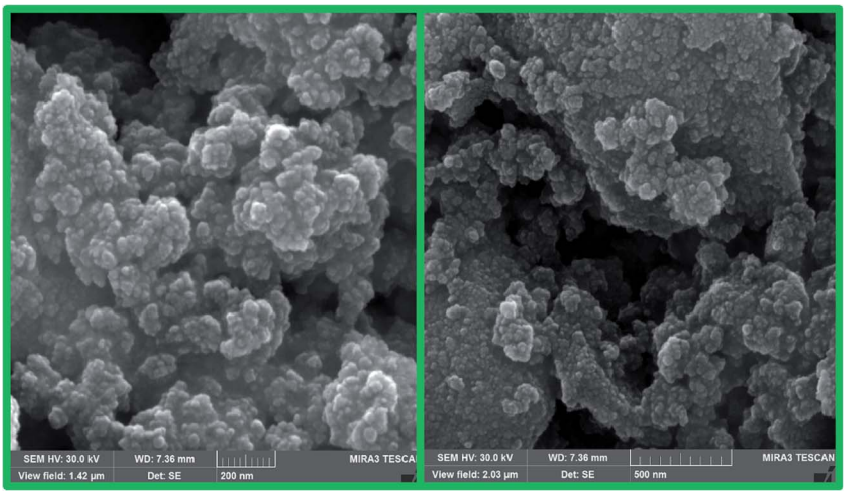

Fig. 6 SEM images of **1a** nanoparticles.

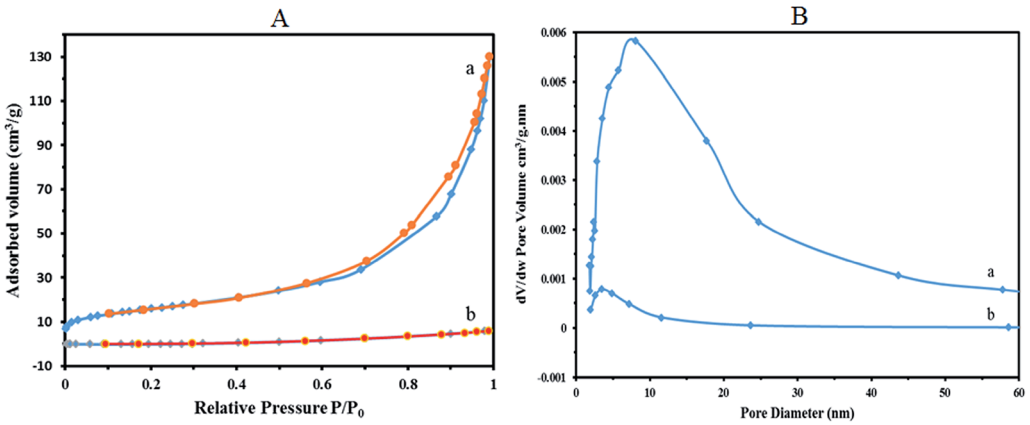

Fig. 7 Nitrogen adsorption–desorption isotherms (A) and pore size distribution (B) of **1a** and **1**.

perfume, polymers and pharmaceuticals.[28–30] This reaction is carried out using active methylene compounds and an aldehyde or a ketone in the presence of a base[29] or Lewis acid as catalysts.[31–35] The bases used as both heterogeneous and homogeneous catalysts. For example, zeolites[36] and hydrotalcites[37] are used under heterogeneous conditions, while ethylenediamine, piperidine or amino acids such as glycine and β-alanine are used under homogeneous conditions.[38,39] The Knoevenagel condensation of benzaldehyde with malononitrile as a model was examined using **1** at 25 °C in water and ethanol. The results are summarized in Table 1 (entries 2 and 5).

The yields of reaction show that **1** is much more effective than the Keggin POMs of $[PW_{12}O_{40}]^{3-}$ (acid or sodium salt) and the mono-lacunary POM of $[PW_{11}O_{39}]^{7-}$ (potassium salt) under similar conditions.[40] The high activity of **1** compared with its similar compounds is attributed to the stannous atoms in **1**. The Knoevenagel condensation catalyzed by **1** in water was carried out with good yields of 85–95% (Table 2). Reaction in absolute ethanol by POM of **1** as a heterogeneous catalyst was also carried out and we found that the products were formed

Table 1 Knoevenagel condensation under various reaction conditions[a]

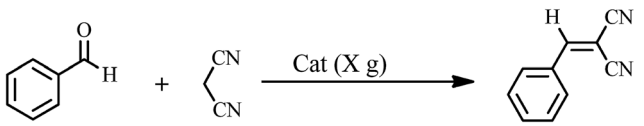

Entry	Cat (X g)	Solvent	Time	Conversion	Yield[b] (%)
1	1 (0.020)	H_2O	1 h	100	85
2	**1 (0.010)**	**H_2O**	**1 h**	**100**	**90**
3	1 (0.0050)	H_2O	2 h	100	85
4	1 (0.020)	EtOH	1 h	100	85
5	**1 (0.010)**	**EtOH**	**1 h**	**100**	**87**
6	1 (0.0050)	EtOH	2 h	100	80
7	Catalyst free	H_2O/EtOH	24 h	40	—

[a] Reaction conditions: benzaldehyde (1 mmol), malononitrile (1.2 mmol), solvent (1 ml), rt, air. [b] Isolated yield.

Table 2 Knoevenagel condensation of aromatic aldehydes with malononitrile[a]

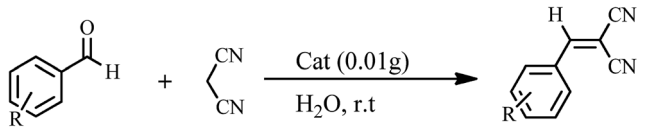

Entry	R	Time (min) cat. **1**	Conversion	Yield[b] (%) cat. **1**
1	4-$CH_3C_6H_4$	80	100	95
2	4-$CH_3OC_6H_4$	10	100	95
3	4-$NO_2C_6H_4$	20	100	95
4	3-$NO_2C_6H_4$	10	100	95
5	4-ClC_6H_4	60	100	92
6	2-ClC_6H_4	60	100	87

[a] Reaction conditions: aromatic aldehyde (1 mmol), malononitrile (1.2 mmol), H_2O (1 ml), rt, air. [b] Isolated yield.

Table 3 Knoevenagel condensation of aromatic aldehydes with malononitrile[a]

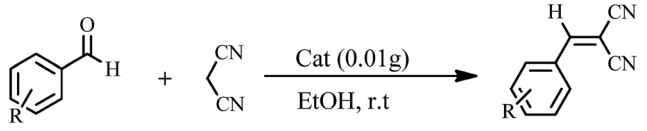

Entry	R	Time (min) cat. **1**	Conversion	Yield[b] (%) cat. **1**
1	4-$CH_3C_6H_4$	80	100	95
2	4-$CH_3OC_6H_4$	60	100	95
3	4-$NO_2C_6H_4$	20	100	95
4	3-$NO_2C_6H_4$	20	100	95
5	4-ClC_6H_4	60	100	90
6	2-ClC_6H_4	30	100	85

[a] Reaction conditions: aromatic aldehyde (1 mmol), malononitrile (1.2 mmol), EtOH (1 ml), rt, air. [b] Isolated yield.

with good yields of 85–95% (Table 3). The catalyst was reused at least five times without any significant decrease in catalytic activities, and the structure of the catalyst remained unchanged after recycling.

Catalytic applications of 1a in the oxidation of sulfides to sulfoxides. As sulfoxides and sulfones are useful synthetic intermediates, the selective oxidation of sulfides to sulfoxides or sulfone is a very important class of reaction in synthetic organic chemistry. Different synthetic methods for the controlled oxidation of conventional sulfides have been previously reported for fundamental transformation. Vanadium Schiff base complexes immobilized on mesoporous silica were used for the oxidation of aromatic sulfides using *tert*-butyl hydroperoxide as an oxidant in acetonitrile by Jain *et al.*[41] Styrene-based peroxotungstate-modified polymer-immobilized ionic liquid-phase catalysts $[PO_4\{WO(O_2)_2\}_4]$@ImPIILP (Im = imidazolium) were synthesized by Doherty *et al.* and used remarkably efficient systems for the selective oxidation of sulfides under mild conditions in batch and continuous flow processes.[42] An alkali exchanged form of mesoporous polytriallylamine and a Cr-grafted material Cr-MPTA-1 were prepared *via* facile *in situ* radical polymerization of a triallylamine template by Bhaumik *et al.* and used successfully as an efficient catalyst for the liquid-phase partial oxidation of sulfides to sulfoxides using H_2O_2 as an oxidant in acetonitrile.[43]

The catalytic activity of **1a** was investigated in the selective oxidation of sulfides to sulfoxides using 30% H_2O_2 as a green oxidant at room temperature. To optimize the reaction condition, methyl phenyl sulfide was used as a model compound. The amount of catalyst and the effect of solvent type were studied on the rate of the reaction (Table 4). The appropriate amount of catalysts needed to carry out the reaction was 0.030 g. As shown in Table 4, solvents H_2O and CH_3CN were examined. The results show that by changing of water to acetonitrile, sulfone was the reaction product indeed of sulfoxide. Owing to the toxicity of acetonitrile, water was selected as a suitable solvent for this purpose. Investigations showed that the oxidation reaction remained incomplete without catalysts under optimized conditions (Table 4, entry 5).

Table 4 Optimization of the reaction conditions with respect to the effect of catalyst and solvent on the oxidation of methyl phenyl sulfide[a]

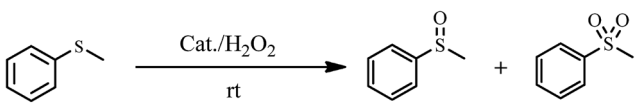

1 **2**

Entry	Cat (mg)	Solvent	Time (min)	Y **1**[b] (%)	Y **2**[b] (%)	Conversion
1	**1a** (10)	MeCN	3 h	—	90	100
2	**1a** (30)	MeCN	60	—	92	100
3	**1a (30)**	**H_2O**	**5**	**90**	**—**	**100**
4	Catalyst free	H_2O	24 h	30	—	—
5	**1** (30)	H_2O	10 h	30	40	—

[a] Reaction conditions: methyl phenyl sulfide (1 mmol), solvent (1.25 ml), H_2O_2 (6 mmol, 30%), rt, air. [b] Isolated yield.

Table 5 Selective oxidation of sulfides to sulfoxides using H_2O_2 catalyzed by **1a**[a]

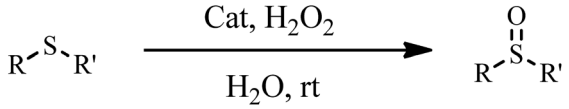

Entry	Catalyst	Substrate	Product	Time (min)	Yield[b] (%)
1	**1a**	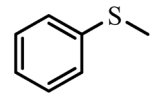	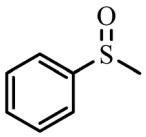	5	90
2	**1a**	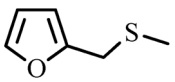	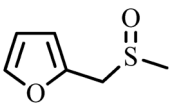	5	95
3	**1a**			5	92
4	**1a**	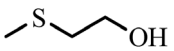	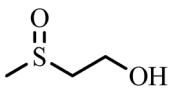	5	90
5	**1a**	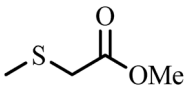	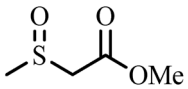	5	95

[a] Reaction conditions: catalyst (30 mg), H_2O_2 (6 mmol, 30%), sulfide (1 mmol), H_2O (1.25 ml) rt, air. [b] Isolated yield.

In order to generalize the scope of the reaction, a series of various sulfides such as benzylic, linear and cyclic sulfides were subjected to the experiment under optimized conditions (Table 5). According to the data listed in Table 5, the reaction was performed in a very short time with high yields. To show the chemoselectivity of this method, the sulfides that contain functional groups such as OH and $COOCH_3$ were subjected to the reaction. The functional groups remained unchanged in the oxidation reaction (Table 5, entries 4 and 5).

The catalytic applications of 1a in the oxidative amination of aldehydes. The importance of amides in organic chemistry is well recognized as they are an integral part of polymers, natural products and pharmaceuticals.[44,45] Hence, a variety of catalytic methods have been developed for the synthesis of amide functionality from aldehydes.[46–48] One of the most common methods of preparing amides is the oxidative amination of aldehydes.[49] Recently, the palladium nanoparticles immobilized on amino functionalized metal–organic framework MIL-

Table 6 Oxidative amidation of aldehydes[a]

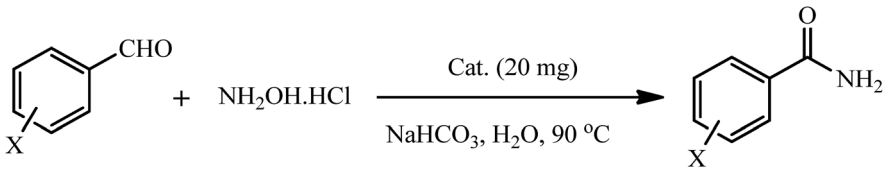

Entry	X	Time (h) cat. **1a**	Conversion	Yield[b] (%)
1	H	3.5	100	94
2	4-Cl	3	100	91
3	4-Me	4	100	90
4	4-NO_2	3	100	96
5	2-NO_2	3.5	100	89
6	2,4-Cl_2	4	100	86

[a] Reaction conditions: aldehyde (1 mmol), hydroxyl amine hydrochloride (1.2 mmol), sodium bicarbonate (1.2 mmol), catalyst (20 mg), and H_2O (1 ml) at 90 °C. [b] Isolated yield.

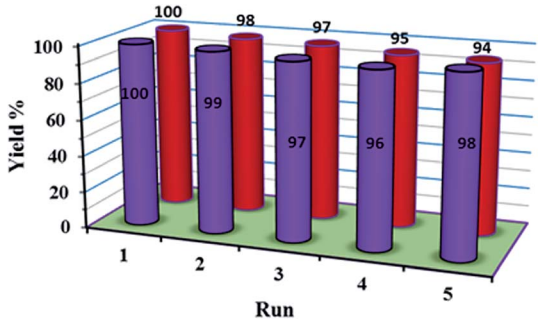

Fig. 8 The recycling experiment of **1a** for the oxidation of methyl phenyl sulfide (blue) and the recycling experiment of **1a** for the oxidation oxidative amination of aldehyde (red).

101(Cr) was used as an active heterogeneous catalyst for the oxidative amination of aldehydes with hydrogen peroxide as an oxidant.[50] In these methods, there are several disadvantages such as the problem of catalyst separation from the reaction mixture and thus less recyclability, harsh conditions and long reaction times.

Thus, $[P_2W_{18}O_{68}(HOSn^{IV}OH)_{32}]^{12-}$ was supported on amine-modified silica-coated magnetite nanoparticles and their catalytic performance was evaluated in the preparation of amides from aldehydes and hydroxylamine hydrochloride in an aqueous medium (Table 6). The products were confirmed by comparison with the literature. As the results show, the catalytic system displayed high performance in the synthesis of active and inactive amides. The reaction time of aldehydes was lower in the presence of electron-withdrawing groups (Table 6, entries 2, 4, 5, 6) than in the presence of electron-donating groups (Table 6, entry 3). Furthermore, the reaction time was affected by the substituted position. For example, the reaction of the *ortho*-derivatives (Table 6, entries 5 and 6) despite having an electron-withdrawing group has a longer reaction time. High product yield, short reaction time, solvent green conditions, facile preparation and reusability of the catalyst are the noteworthy advantages that make the present catalytic protocol superior to those reported previously.

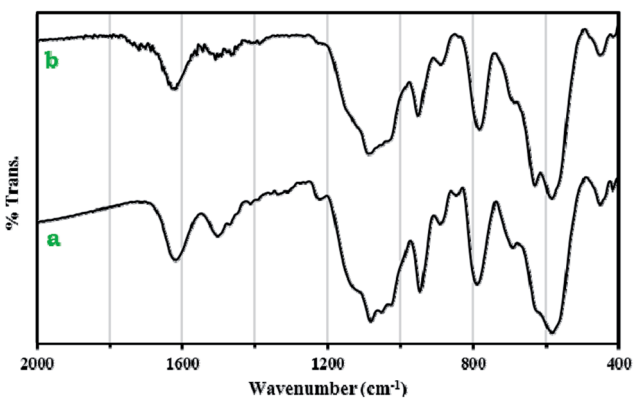

Fig. 9 The FT-IR spectra of **1a** nanoparticles (a) and **1a** nanoparticles after five consecutive runs (b).

Catalysts recovery and reuse

The recycling and stability of the catalyst were investigated. The catalyst could be easily recovered using an external magnet and further recycled. The recovered catalyst after the first use was washed thoroughly with ether and reused in a subsequent reaction. The strong coordination of POM with functionalized Fe_3O_4 magnetite nanoparticles makes the catalyst stable, nearly free from leaching, and reusable for a greater number of cycles (five times, (Fig. 8)). The FT-IR spectra showed no significant structural changes for the catalyst after five consecutive runs (Fig. 9).

Conclusion

In summary, heteropolytungstostannate of $K_{11}H[P_2W_{18}O_{68}(HOSn^{IV}OH)_3]\cdot H_2O$ (**1**) was used as a heterogeneous and homogeneous catalyst in the high selectivity and efficient Knoevenagel condensation and for fabrication of magnetically recoverable catalyst *via* electrostatic interaction. The new type of magnetically recoverable nanocomposite was characterized using IR, SEM, XRD, EDX and AGFM. The magnetically recoverable nanocatalyst is utilized as a high-selectivity and efficient catalyst in the oxidation of sulfides to sulfoxides and the oxidative amination of aldehydes. The catalyst could be easily separated from the reaction mixture and used for the next run over five times without any obvious decrease in the catalytic activity.

Conflicts of interest

The authors declare that they have no competing interests.

References

1 M. T. Pope, *Heteropoly and Isopoly Oxometalate*, Springer-Verlag, Berlin, 1983, p. 31.
2 U. Kortz, M. G. Savelieff, B. S. Bassil and M. H. Dickman, *Angew. Chem., Int. Ed.*, 2001, **40**, 3384.
3 V. W. Day and W. G. Klemperer, *Science*, 1985, **228**, 533.
4 C. L. Hill and C. M. Prosser-McCartha, *Coord. Chem. Rev.*, 1995, **143**, 407.
5 I. V. Kozhevnikov, *Chem. Rev.*, 1998, **98**, 171.
6 N. Mizuno and M. Misono, *Chem. Rev.*, 1998, **98**, 199.
7 X. M. Yan, J. H. Lei, D. Liu, Y. C. Wu and W. Liu, *Mater. Res. Bull.*, 2007, **42**, 1905.
8 N. Dubey, S. S. Rayalu, N. K. Labhsetwar and S. Devotta, *Int. J. Hydrogen Energy*, 2008, **33**, 5958.
9 M. A. Alibeik, Z. Zaghaghi and I. M. Baltork, *J. Chin. Chem. Soc.*, 2008, **55**, 1.
10 S. Uchida and N. Mizuno, *J. Am. Chem. Soc.*, 2004, **126**, 1602.
11 N. M. Okun, M. D. Ritorto, T. M. Anderson, R. P. Apkarian and C. L. Hill, *Chem. Mater.*, 2004, **16**, 2551.
12 C. W. Lim and I. S. Lee, *Nano Today*, 2010, **5**, 412.
13 K. K. Senapati, C. Borgohain and P. Phukan, *J. Mol. Catal. A: Chem.*, 2011, **339**, 24.

14 M. G. Egusquiza, C. I. Cabello, I. L. Botto, H. J. Thomas, S. Casuscelli, E. Herrero and D. Gazzoli, *Catal. Commun.*, 2012, **26**, 117.
15 A. Patel and K. Patel, *Inorg. Chim. Acta*, 2014, **419**, 130.
16 V. Nardello, J. M. Aubry, D. E. D. Vos, R. Neumann, W. Adam, R. Zhang, J. E. Elshof, P. T. Witte and P. L. Alsters, *J. Mol. Catal. A: Chem.*, 2006, **251**, 185.
17 I. C. M. S. Santos, J. A. F. Gamelas, M. S. S. Balula, M. M. Q. Simoes, M. G. P. M. S. Neves, J. A. S. Cavaleiro and A. M. V. Cavaleiro, *J. Mol. Catal. A: Chem.*, 2007, **262**, 41.
18 F. Xin and M. T. Pope, *J. Am. Chem. Soc.*, 1996, **118**, 7731.
19 R. Khshnavazi and L. Bahrami, *J. Coord. Chem.*, 2009, **62**, 2067.
20 W. H. Knoth, P. J. Domaille and R. L. Harlow, *Inorg. Chem.*, 1986, **25**, 1577.
21 X. Liu, Z. Ma, J. Xing and H. Liu, *J. Magn. Magn. Mater.*, 2004, **270**, 1.
22 M. Yamaura, R. L. Camilo, L. C. Sampaio, M. A. Macedo, M. Nakamura and H. E. Toma, *J. Magn. Magn. Mater.*, 2004, **279**, 210.
23 F. Shahbazi and K. Amani, *Catal. Commun.*, 2014, **55**, 57.
24 A. Alizadeh, M. M. Khodaei, M. Beygzadeh, D. Kordestani and M. Feyzi, *Bull. Korean Chem. Soc.*, 2012, **33**, 2546.
25 H. Ono and T. Katsumata, *Appl. Phys. Lett.*, 2001, **78**, 1832.
26 F. An and B. Gao, *J. Hazard. Mater.*, 2007, **145**, 495.
27 Y. Lin, H. Chen, K. Lin, B. Chen and C. Chiou, *J. Environ. Sci.*, 2011, **23**, 44.
28 (*a*) G. Jones, *Org. React.*, 1967, **15**, 204; (*b*) L. F. Tietze and U. Beifuss, in *Comprehensive Organic Synthesis*, Pergamon, New York, 1991, vol. 2, p. 341.
29 F. Bigi, L. Chesini, R. Maggi and G. Sartori, *J. Org. Chem.*, 1999, **64**, 1033.
30 N. Yu, J. M. Aramini, M. W. German and Z. Huang, *Tetrahedron Lett.*, 2000, **41**, 6993.
31 (*a*) D. S. Bose and A. V. Narsaiah, *J. Chem. Res.*, 2001, 36; (*b*) J. L. Scott and C. L. Raston, *Green Chem.*, 2000, **2**, 245.
32 (*a*) W. Lehnert, *Tetrahedron*, 1974, **30**, 301; (*b*) B. Green, R. I. Crane, I. S. Khaidem, R. S. Leighton, S. S. Newaz and T. E. Smyser, *J. Org. Chem.*, 1985, **50**, 640.
33 P. Shanthan Rao and R. V. Venkataratnam, *Tetrahedron Lett.*, 1991, **32**, 5821.
34 G. Bartoli, R. Beleggia, S. Giuli, A. Giuliani, E. Marcantoni, M. Massaccesi and M. Paletti, *Tetrahedron Lett.*, 2006, **47**, 6501.
35 S. Kantevari, R. Bantu and L. Nagarapu, *J. Mol. Catal. A: Chem.*, 2007, **269**, 53.
36 (*a*) S. Saravanamurugan, M. Palanichamy, M. Hartmann and V. Murugesan, *Appl. Catal., A*, 2006, **298**, 8; (*b*) T. I. Reddy and R. S. Varma, *Tetrahedron Lett.*, 1997, **38**, 1721.
37 M. L. Kantam, B. M. Choudary, C. V. Reddy, K. K. Rao and F. Figueras, *Chem. Commun.*, 1998, 1033.
38 (*a*) C. F. H. Allen and F. W. Spangler, *Org. Syn. Coll.*, 1955, **3**, 377; (*b*) L. Rand, J. V. Swisher and C. J. Cronin, *J. Org. Chem.*, 1962, **27**, 3505.
39 (*a*) D. S. Acker and W. R. Hertler, *J. Am. Chem. Soc.*, 1962, **84**, 3370; (*b*) G. Cardillo, S. Fabbroni, L. Gentilucci, M. Gianotti and A. Tolomelli, *Synth. Commun.*, 2003, **33**, 1587.
40 S. Zhao, Y. Chen and Y. F. Song, *Appl. Catal., A*, 2014, **475**, 140.
41 S. L. Jain, B. S. Rana, B. Singh, A. K. Sinha, A. Bhaumik, M. Nandi and B. Sain, *Green Chem.*, 2010, **12**, 374.
42 S. Doherty, J. G. Knight, M. A. Carroll, A. R. Clemmet, J. R. Ellison, T. Backhouse, N. Holmes and R. A. Bourne, *RSC Adv.*, 2016, **6**, 73118.
43 N. Salam, P. Mondal, J. Mondal, A. S. Roy, A. Bhaumik and S. M. Islam, *RSC Adv.*, 2012, **2**, 6464.
44 J. M. Humphery and A. R. Chamberlin, *Chem. Rev.*, 1997, **97**, 2243.
45 R. K. Mylavarapu, G. C. M. Kondaiah, N. Kolla, R. Veeramalla, P. Koilkonda, A. Bhattacharya and R. Bandnewichhor, *Org. Process Res. Dev.*, 2007, **11**, 1065.
46 W. J. Yoo and C. J. Li, *J. Am. Chem. Soc.*, 2006, **128**, 13064.
47 J. Liang, J. Lv and Z. Shang, *Tetrahedron*, 2011, **67**, 8532.
48 S. C. Ghosh, J. S. Y. Ngiam, C. L. L. Chai, A. M. Seayad, T. T. Dang and A. Chen, *Adv. Synth. Catal.*, 2012, **354**, 1407.
49 (*a*) A. M. Asencio, M. Yus and D. J. Ramon, *Tetrahedron*, 2012, **68**, 3948; (*b*) M. A. Ali and T. Punniyamurthy, *Adv. Synth. Catal.*, 2010, **352**, 288; (*c*) K. Yamaguchi, H. Kobayashi, Y. Wang, T. Oishi, Y. Ogasawara and N. Mizuno, *Catal. Sci. Technol.*, 2013, **3**, 318; (*d*) R. Vanjari, T. Guntreddi and K. N. Singh, *Green Chem.*, 2014, **16**, 351.
50 M. Saikia and L. Saikia, *RSC Adv.*, 2016, **6**, 14937.